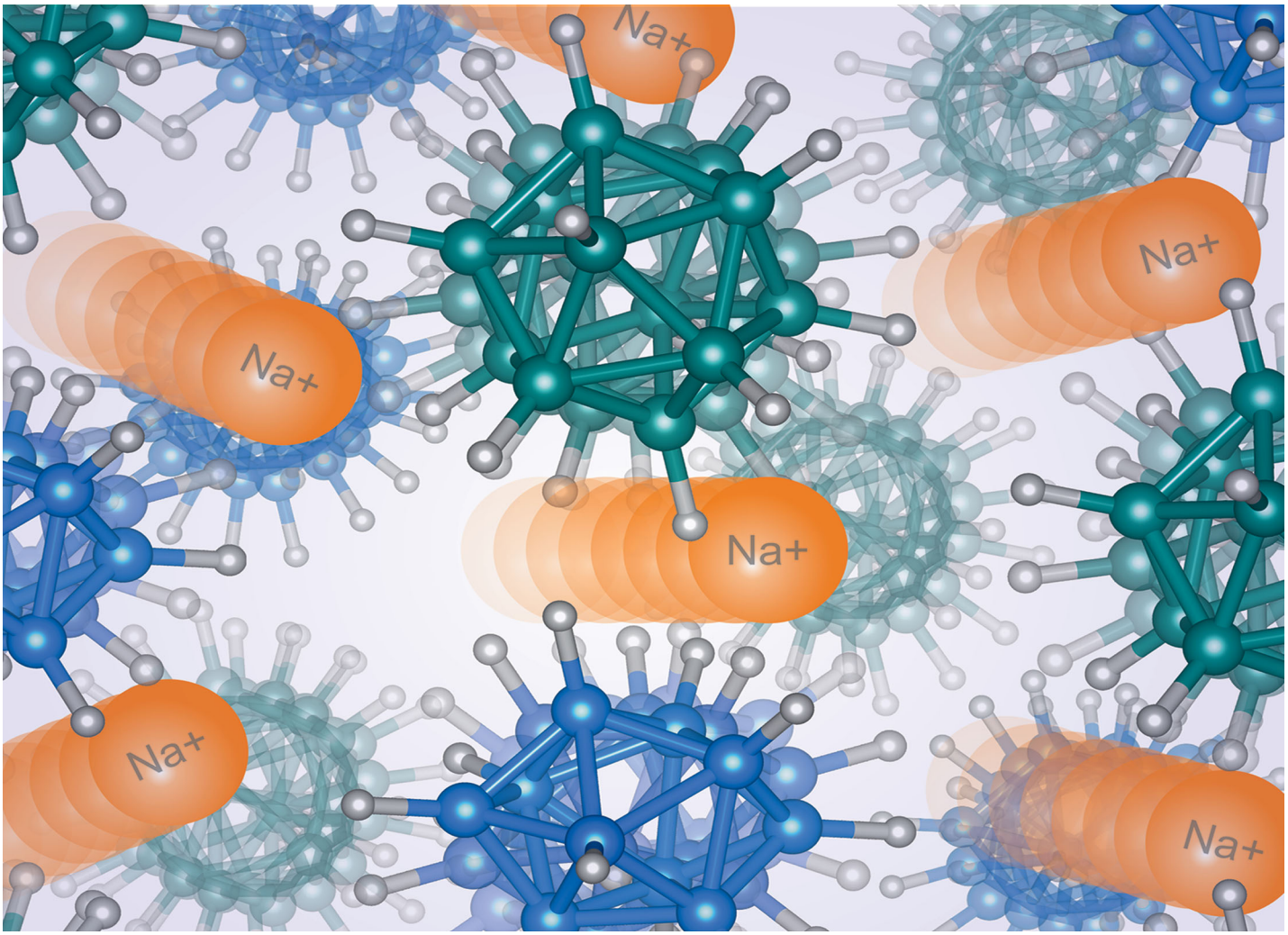

Showcasing research from Léo Duchêne *et al.*, resulting from a collaboration between the Swiss Federal Laboratories for Materials Science and Technology and the University of Geneva, Switzerland

A highly stable sodium solid-state electrolyte based on a dodeca/deca-borate equimolar mixture

Fast rotating and highly stable *closo*-borate anions enable fast and stable sodium cycling in $Na_2(B_{12}H_{12})_{0.5}(B_{10}H_{10})_{0.5}$, a new promising solid electrolyte.

As featured in:

See A. Remhof *et al.*, *Chem. Commun.*, 2017, **53**, 4195.

ROYAL SOCIETY OF CHEMISTRY

rsc.li/chemcomm

Registered charity number: 207890

ChemComm

COMMUNICATION

View Article Online
View Journal | View Issue

Cite this: *Chem. Commun.*, 2017, 53, 4195

Received 30th January 2017,
Accepted 22nd March 2017

DOI: 10.1039/c7cc00794a

rsc.li/chemcomm

A highly stable sodium solid-state electrolyte based on a dodeca/deca-borate equimolar mixture†

L. Duchêne,[ab] R.-S. Kühnel,[a] D. Rentsch,[a] A. Remhof,*[a] H. Hagemann[b] and C. Battaglia[a]

$Na_2(B_{12}H_{12})_{0.5}(B_{10}H_{10})_{0.5}$, a new solid-state sodium electrolyte is shown to offer high Na^+ conductivity of 0.9 mS cm^{-1} at 20 °C, excellent thermal stability up to 300 °C, and a large electrochemical stability window of 3 V including stability towards sodium metal anodes, all essential prerequisites for a stable room-temperature 3 V all-solid-state sodium-ion battery.

All-solid-state sodium-ion batteries promise to simultaneously yield better performance and lower cost as compared to state-of-the-art lithium-ion technology using organic liquid electrolytes.[1,2] To build such a competitive all-solid-state battery requires a solid-state electrolyte (SSE) with high ionic conductivity near room temperature and high thermal and electrochemical stability. Meeting these three requirements simultaneously still represents a major challenge. High ionic conductivity of or above 10^{-3} S cm^{-1} has been reached in oxide ceramics or more recently in sulfide phases but these materials still suffer from high electrode–electrolyte interface resistance or intrinsically small electrochemical stability windows of 1 V or less, respectively.[3–10] Recently, complex hydride materials and particularly metal *closo*-borates have emerged as promising alternative SSEs.[11,12] Metal *closo*-borates are salts with polyhedral $B_nH_n^{2-}$ (n = 6–12) anions, among which the salts of the $B_{10}H_{10}^{2-}$ and $B_{12}H_{12}^{2-}$ anions were early noted due to their high thermal and chemical stability.[13] $LiCB_{11}H_{12}$ as a halogen free electrolyte was also predicted by theory[14] and used in experiments to synthesize a Mg-electrolyte.[15] *closo*-Borate and related carborate salts (with monovalent $CB_{n-1}H_n^-$ anions) also exhibit structural transitions to highly conductive phases, above room temperature.[16–19] Strategies to stabilize these superionic phases at room temperature and below, including mechanical milling and cation or anion substitutions, have been implemented.[20–23] Yet, studies on *closo*-borates have focused almost exclusively on improving conductivity, while only preliminary work has been performed on the assessment of their electrochemical stability window and of their suitability for integration into a battery. Here, we report a new sodium superionic conductor $Na_2(B_{12}H_{12})_{0.5}(B_{10}H_{10})_{0.5}$ with a conductivity close to 10^{-3} S cm^{-1} at room temperature (20 °C). We further demonstrate that this material is compatible with a sodium metal anode and fulfils all prerequisites to be used in a 3 V all-solid-state sodium-ion battery.

Fig. 1a shows differential scanning calorimetry (DSC) data for the individual precursors $Na_2B_{12}H_{12}$ and $Na_2B_{10}H_{10}$ and their reacted 1 : 1 equimolar mixture. Both precursors show a characteristic endothermic peak at the temperature of their respective structural phase transition, as previously described.[24,25] No such event is observed for the 1 : 1 mixture indicating that $Na_2(B_{12}H_{12})_{0.5}(B_{10}H_{10})_{0.5}$ does not undergo a phase transition within this temperature window. Besides the first heating cycle, we also show DSC data of the third heating cycle, which almost coincides with the first cycle, and demonstrates the stability of the equimolar

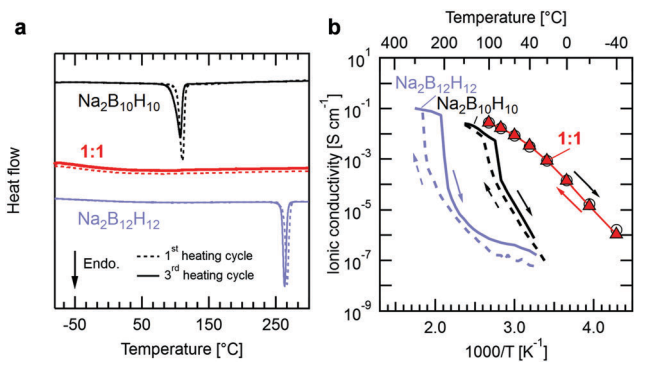

Fig. 1 (a) DSC data for pure $Na_2B_{12}H_{12}$, $Na_2B_{10}H_{10}$ and their equimolar 1 : 1 mixture, $Na_2(B_{12}H_{12})_{0.5}(B_{10}H_{10})_{0.5}$. (b) Temperature-dependent Na^+ conductivity for pure $Na_2B_{12}H_{12}$, $Na_2B_{10}H_{10}$[16,17] and $Na_2(B_{12}H_{12})_{0.5}(B_{10}H_{10})_{0.5}$. Empty circles and filled triangles shown for the 1 : 1 mixture are measurement points upon heating and cooling, respectively.

[a] *Empa, Swiss Federal Laboratories for Materials Science and Technology, CH-8600 Dübendorf, Switzerland. E-mail: arndt.remhof@empa.ch*
[b] *Département de Chimie-Physique, Université de Genève, CH-1211 Geneva 4, Switzerland*

† Electronic supplementary information (ESI) available: Experimental details and supplementary figures. See DOI: 10.1039/c7cc00794a

mixture when subjected to thermal cycling. Thermal characterization was also carried out for intermediate $Na_2(B_{12}H_{12})_{1-x}(B_{10}H_{10})_x$ compositions ($0.1 < x < 0.6$, see Fig. S1, ESI†) for which the endothermic peaks are still visible but decrease in size and ultimately vanish as the ratio approaches $x = 0.5$, at which the precursors fully react.

Fig. 1b presents the ionic conductivity of $Na_2(B_{12}H_{12})_{0.5}(B_{10}H_{10})_{0.5}$ determined by impedance spectroscopy as a function of temperature (see Experimental section and Fig. S2, ESI,† for details). The conductivities of $Na_2B_{12}H_{12}$ and $Na_2B_{10}H_{10}$ obtained by Udovic *et al.*[16,17] are also reported for comparison. The room temperature ionic conductivity for the equimolar ratio is several orders of magnitude higher than that of $Na_2B_{12}H_{12}$ and $Na_2B_{10}H_{10}$, reaching 0.9 mS cm^{-1} at 20 °C. This value is comparable to typical conductivities reported for oxide and sulfide electrolytes[3–8] and only slightly lower than that of a standard sodium liquid electrolyte based on 1 M $NaClO_4$ dissolved in EC:PC (3.3 mS cm^{-1} at 25 °C,[26] assuming a sodium transference number of 0.4). Within the family of complex hydrides, this conductivity is comparable to the recently reported $Na_3BH_4B_{12}H_{12}$ and highly conducting, ball-milled $Na_2B_{12}H_{12}$[21,22] and is only surpassed by equimolar mixed carborate phases that can reach exceptional conductivity of 70 mS cm^{-1} at room temperature[23] but have yet to demonstrate their applicability as SSEs in all-solid-state batteries. Similarly to the observed thermal behavior, the equimolar mixture shows no signs of a phase transition in the temperature-dependent conductivity data, whilst the conductivity of the precursors drops sharply at the onset temperatures at which latent heat is observed in DSC. Consequently, while hysteresis in conductivity is observed for both precursors upon temperature cycling, the conductivity of the equimolar mixture shows no hysteresis between heating and cooling. Still, the activation energy for Na^+ diffusion in $Na_2(B_{12}H_{12})_{0.5}(B_{10}H_{10})_{0.5}$ decreases smoothly from 0.7 at −40 °C to 0.4 eV at 100 °C with increasing temperature. A similar behavior was observed for carborate mixtures[23] and $Na_3BH_4B_{12}H_{12}$[21] and attributed to temperature dependent anion dynamics within the respective crystal structures. The connection between lattice parameter, anion dynamics and the evolution of cation conductivity in *closo*-borates was also recently discussed by Varley *et al.* based on *ab initio* molecular dynamics calculations.[27]

Crystal structure and lattice parameters were determined by X-ray diffraction (XRD). In Fig. 2a we compare the diffractograms of the equimolar mixture at room temperature with the ones of the precursors in their respective high temperature (HT) conductive phases, *i.e.* body-centered cubic (bcc) $Na_2B_{12}H_{12}$ at 300 °C and face-centered cubic (fcc) $Na_2B_{10}H_{10}$ at 180 °C. At room temperature the precursors show additional reflections indicative of the lower structure symmetry below the phase transition (see Fig. S3a, ESI†). We find that the reflections in the XRD pattern of the mixed phase can all be matched to the one of $Na_2B_{10}H_{10}$ in its HT fcc phase. We conclude that the equimolar mixture stabilizes a single phase, isostructural to the highly conducting HT phase of $Na_2B_{10}H_{10}$. Refinement yields a slightly larger unit cell parameter of a = 10.029 Å for $Na_2(B_{12}H_{12})_{0.5}(B_{10}H_{10})_{0.5}$ at room temperature *vs.* a = 9.854 Å for $Na_2B_{10}H_{10}$ at 180 °C (see Fig. S3b and c, ESI†). Additionally, XRD

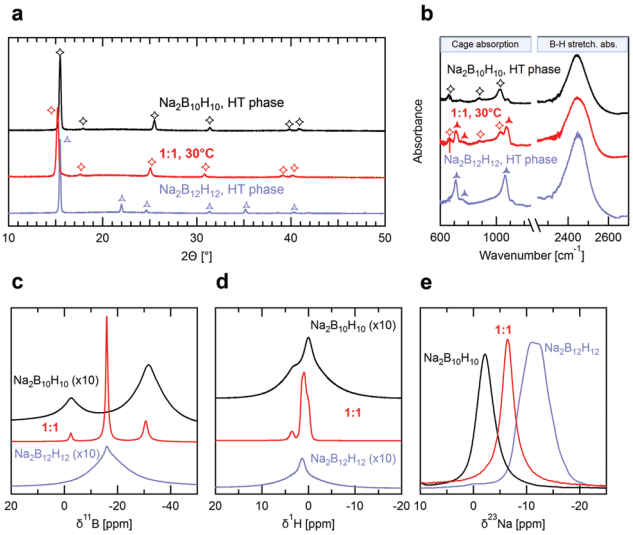

Fig. 2 (a) XRD patterns and (b) infrared spectra of the HT phases of $Na_2B_{12}H_{12}$ and $Na_2B_{10}H_{10}$ recorded at 300 and 180 °C, respectively, compared to the room temperature phase of $Na_2(B_{12}H_{12})_{0.5}(B_{10}H_{10})_{0.5}$. Characteristic features are marked by symbols. (c–e) Room temperature ^{1}H, ^{11}B and ^{23}Na MAS solid-state NMR spectra of $Na_2B_{12}H_{12}$, $Na_2B_{10}H_{10}$ and $Na_2(B_{12}H_{12})_{0.5}(B_{10}H_{10})_{0.5}$. For the ^{1}H and ^{11}B NMR data, the $Na_2B_{12}H_{12}$ and $Na_2B_{10}H_{10}$ spectra were Y-offset and up-scaled by a factor of 10 to facilitate data comparison.

measurements of $Na_2(B_{12}H_{12})_{0.5}(B_{10}H_{10})_{0.5}$ at 300 °C (see Fig. S3a, ESI†) show no structural change other than an expansion of the unit cell parameters, demonstrating again the high thermal stability in agreement with DSC and conductivity measurements. Note that equimolar mixtures of $Na_2B_{12}H_{12}$ and $Na_2B_{10}H_{10}$ were recently reported by Tang *et al.*,[22] who also used mechanical milling followed by a heat treatment at 275 °C for 16 h. However, their mixture still contained predominantly (>70%) the low temperature (LT) phase of $Na_2B_{12}H_{12}$ as refined from XRD, indicating only partial conversion to the mixed phase, and no conductivity measurement was reported. Our results prove that using appropriate reaction conditions, equimolar mixtures of $Na_2B_{12}H_{12}$ and $Na_2B_{10}H_{10}$ fully react and stabilize a single mixed-anion phase.

To gain insight into the local anion configuration in the mixed-anion structure, we performed infrared (IR) spectroscopy measurements. Fig. 2b compares the IR spectra of the HT phases of both $Na_2B_{12}H_{12}$ (300 °C) and $Na_2B_{10}H_{10}$ (180 °C) with $Na_2(B_{12}H_{12})_{0.5}(B_{10}H_{10})_{0.5}$ at room temperature. For both precursors, B–H stretching and cage absorption modes are identified in the wavenumber ranges of 2400–2500 cm^{-1} and 600–1200 cm^{-1}, respectively. These characteristic absorption modes correspond to those previously assigned in the IR spectra of $B_{10}H_{10}^{2-}$ and $B_{12}H_{12}^{2-}$ measured in solution,[13,28] characteristic of the respective D_{4d} and I_h point group symmetry of these ions. Recent theoretical DFT calculations confirm these assignments.[29] In the LT phases of $Na_2B_{12}H_{12}$ and $Na_2B_{10}H_{10}$ (see Fig. S4, ESI†) significant splitting of the absorption modes can be seen, indicative of a lowered symmetry of the ions, whereas the anions in the HT phases adopt a similar symmetry than in the solution. Therefore, we conclude that they sit in a very symmetric environment that is a consequence

of the cubic symmetry of the crystal structure and of the absence of a preferred orientation of the anions, *i.e.* of rotational disorder. The IR spectrum of $Na_2(B_{12}H_{12})_{0.5}(B_{10}H_{10})_{0.5}$ at room temperature corresponds closely to the sum of the spectra of $Na_2B_{12}H_{12}$ and $Na_2B_{10}H_{10}$ in their respective HT phases and all vibration modes can be assigned to the two *closo*-borate anions. This shows that both $B_{10}H_{10}^{2-}$ and $B_{12}H_{12}^{2-}$ are still present in the structure and suggests either an average of rotationally disordered but static configurations, or of dynamic rotation of the anions.

To distinguish between these two cases, we recorded solid-state ^{11}B, ^{1}H and ^{23}Na magic-angle spinning nuclear magnetic resonance (MAS NMR) spectra of $Na_2B_{12}H_{12}$, $Na_2B_{10}H_{10}$ and their 1 : 1 mixture. All samples were measured at room temperature to compare the ion dynamics. As seen from comparison in Fig. 2c–e, the spectrum of the equimolar mixture comprises all the resonances of the constituents in the precursors. Importantly, the resonances of the equimolar mixture are all considerably narrowed compared to the signals of the pure precursors, especially in the case of boron and hydrogen (Fig. 2c–e). This narrowing is a sign of fast dynamics of the ions in the 1 : 1 mixture compared to the borate starting materials. We may thus also interpret the IR data as a result of fast anion dynamics rather than an average of frozen configurations. Additionally, since X-ray diffraction already showed that $Na_2(B_{12}H_{12})_{0.5}(B_{10}H_{10})_{0.5}$ has a well-defined crystal structure, we can conclude that this motion is rotational and not translational (see Fig. 3), as previously suggested based on NMR and quasi-elastic neutron scattering experiments on other *closo*-borates.[30,31] ^{11}B NMR also confirms that the $B_{12}H_{12}^{2-}$ and $B_{10}H_{10}^{2-}$ anions remain intact in $Na_2(B_{12}H_{12})_{0.5}(B_{10}H_{10})_{0.5}$ with no significant ^{11}B signal intensity detectable other than the ones of the *closo*-borate anions. The 1 : 1 $B_{12}H_{12}^{2-}$ to $B_{10}H_{10}^{2-}$ ratio was verified by ^{11}B solution-state NMR by dissolving $Na_2(B_{12}H_{12})_{0.5}(B_{10}H_{10})_{0.5}$ in deuterated water, and it was confirmed that both anions are indeed present in a 1 : 1 molar ratio (see Fig. S5, ESI†). Finally, it can be seen in Fig. 2e that the ^{23}Na NMR chemical shift and thus the sodium environment in $Na_2(B_{12}H_{12})_{0.5}(B_{10}H_{10})_{0.5}$ is averaged between that of $Na_2B_{10}H_{10}$ and $Na_2B_{12}H_{12}$, supporting the hypothesis of a solid solution phase, as depicted in Fig. 3.

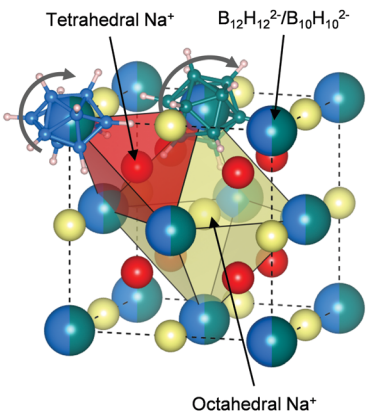

Fig. 3 Simplified structure of $Na_2(B_{12}H_{12})_{0.5}(B_{10}H_{10})_{0.5}$ based on the HT phase of $Na_2B_{10}H_{10}$. Partially occupied Na^+ ions sites are shown in different colors to distinguish tetrahedral and octahedral coordination. $B_{12}H_{12}^{2-}$ and $B_{10}H_{10}^{2-}$ anions are randomly distributed in the fcc framework. Two example anions are shown.

To evaluate the suitability of $Na_2(B_{12}H_{12})_{0.5}(B_{10}H_{10})_{0.5}$ as SSE in an all-solid-state sodium-ion battery, we performed cyclic voltammetry tests at room temperature. Fig. 4a shows current density *vs.* voltage measured for a $Na|Na_2(B_{12}H_{12})_{0.5}(B_{10}H_{10})_{0.5}|Pt$ cell cycled at voltages between −0.5 V and 6.5 V at 0.1 mV s^{-1}. Near 0 V, we observed characteristic anodic and cathodic current peaks associated with sodium stripping and plating. Towards higher voltages, the current density remains low up to 6.5 V but first oxidation currents were observed in the nA cm^{-2} range. We therefore built two additional cells for a precise measure of the electrochemical stability window of $Na_2(B_{12}H_{12})_{0.5}(B_{10}H_{10})_{0.5}$. To determine its oxidative stability, a platinum working electrode (WE) was swept against a sodium counter electrode from the open-circuit voltage of 1.6 V up to a voltage of 5.5 V at a slow rate of 0.1 mV s^{-1} to remain near equilibrium. Results are shown in Fig. 4b. Small currents indicative of slow electrolyte oxidation can be measured for cell voltages above 3 V but remain below 10 nA cm^{-2} at higher voltages. To determine the reductive stability, an aluminum working electrode, which unlike platinum does not alloy with sodium, was preferred. Starting at the cell's open circuit voltage of 1.6 V, the voltage was swept down to −0.5 V. On aluminum, no reduction currents are observed down to 0 V, below which the sodium plating peak appears, suggesting that the electrolyte is stable in contact with metallic sodium.

We conclude that $Na_2(B_{12}H_{12})_{0.5}(B_{10}H_{10})_{0.5}$ offers a practical electrochemical stability window of 3 V, most likely limited by

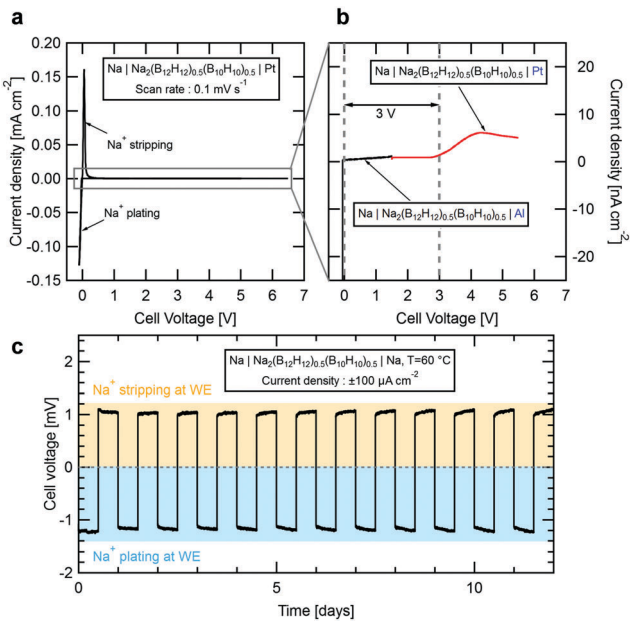

Fig. 4 Room temperature cyclic voltammogram of (a) a $Na|Na_2(B_{12}H_{12})_{0.5}(B_{10}H_{10})_{0.5}|Pt$ cell from −0.5 to 6.5 V at a scan rate of 0.1 mV s^{-1} and (b) of $Na|Na_2(B_{12}H_{12})_{0.5}(B_{10}H_{10})_{0.5}|Al$ & $Na|Na_2(B_{12}H_{12})_{0.5}(B_{10}H_{10})_{0.5}|Pt$ cells between −0.5 and 5.5 V showing the oxidative (red) and reductive (black) stability of the electrolyte, respectively. (c) Galvanostatic cycling of a symmetric $Na|Na_2(B_{12}H_{12})_{0.5}(B_{10}H_{10})_{0.5}|Na$ cell at 60 °C with a current density of 100 µA cm^{-2}.

oxidation of the $B_{10}H_{10}^{2-}$ anions.[32] Preliminary cyclic voltammetry measurements performed on other *closo*-borate electrolytes suggested a much larger stability window for this class of compounds.[17,21,22] However, we believe that the stability has been over-estimated due to the very small oxidation currents that may not have been detected in previous measurements. In fact, Han *et al.*[33] recently discussed the limitation of conventional cyclic voltammetry measurements to evaluate the true stability window of solid-state electrolytes. This limitation can be overcome only if one is able to measure very small currents (we used a low current channel with pA resolution) or by artificially increasing the contact area between the electrolyte and the working electrode.

To further confirm the compatibility with a sodium metal anode, we built a symmetric $Na|Na_2(B_{12}H_{12})_{0.5}(B_{10}H_{10})_{0.5}|Na$ cell which was galvanostatically cycled at 60 °C. Fig. 4c shows the evolution of the cell voltage over time as sodium is plated and stripped at a current of ± 100 μA cm^{-2} in intervals of 12 h. Our results demonstrate that sodium is plated and stripped fully reversibly with a low combined over-potential reaching a maximum of 1.2 mV, in good agreement with the measured conductivity for the electrolyte at 60 °C. Importantly, the overall voltage remains stable for 12 days confirming that the electrolyte is not degrading. Note that during a 12 h cycle, a charge equivalent of 1.2 mA h cm^{-2} is cycled through the material. Considering a typical sodium cathode material with a capacity of 120 mA h g^{-1} and a mass loading of 20 mg, each 12 h cycle of this measurement corresponds to 50% of a full charge.

In conclusion, we demonstrated that among SSEs with comparable conductivity, $Na_2(B_{12}H_{12})_{0.5}(B_{10}H_{10})_{0.5}$ stands out as a particularly stable material, notably when compared to sulphide phases. The electrochemical stability window of 3 V is compatible with high performance sodium cathode materials such as Na_2FePO_4F, $NaCrO_2$. We further demonstrated that $Na_2(B_{12}H_{12})_{0.5}(B_{10}H_{10})_{0.5}$ is compatible with a sodium metal anode enabling long-term and reversible sodium plating and stripping. We also believe that further anion engineering *e.g.* by mixing larger halogenated *closo*-borates with a lower charge density, could yield even higher stability and conductivity and that this class of materials holds promise for competitive high voltage all-solid-state sodium-ion batteries.

We would like to thank the Swiss National Science Foundation for financial support within the Sinergia project 'Novel ionic conductors' under contract number CRSII2_160749/1. The NMR hardware was partially granted by the Swiss National Science Foundation (SNFS, grant no. 206021_150638/1).

Notes and references

1 J. Janek and W. G. Zeier, *Nat. Energy*, 2016, **1**, 16141.
2 D. Kundu, E. Talaie, V. Duffort and L. F. Nazar, *Angew. Chem., Int. Ed.*, 2015, **54**, 3432.
3 H. Engstrom, J. B. Bates, W. E. Brundage and J. C. Wang, *Solid State Ionics*, 1981, **2**, 265.
4 J. B. Goodenough, H. Y.-P. Hong and J. A. Kafalas, *Mater. Res. Bull.*, 1976, **11**, 203.
5 A. Hayashi, K. Noi, A. Sakuda and M. Tatsumisago, *Nat. Commun.*, 2012, **3**, 856.
6 L. Zhang, K. Yang, J. Mi, L. Lu, L. Zhao, L. Wang, Y. Li and H. Zeng, *Adv. Energy Mater.*, 2015, **5**, 2.
7 A. Banerjee, K. H. Park, J. W. Heo, Y. J. Nam, C. K. Moon, S. M. Oh, S.-T. Hong and Y. S. Jung, *Angew. Chem., Int. Ed.*, 2016, **55**, 9634.
8 W. D. Richards, L. J. Miara, Y. Wang, J. C. Kim and G. Ceder, *Chem. Mater.*, 2016, **28**, 266.
9 W. D. Richards, T. Tsujimura, L. J. Miara, Y. Wang, J. C. Kim, S. P. Ong, I. Uechi, N. Suzuki and G. Ceder, *Nat. Commun.*, 2016, **7**, 11009.
10 I.-H. Chu, C. S. Kompella, H. Nguyen, Z. Zhu, S. Hy, Z. Deng, Y. S. Meng and S. P. Ong, *Sci. Rep.*, 2016, **6**, 33733.
11 R. Mohtadi, A. Remhof and P. Jena, *J. Phys.: Condens. Matter*, 2016, **28**, 353001.
12 B. R. S. Hansen, M. Paskevicius, H.-W. Li, E. Akiba and T. R. Jensen, *Coord. Chem. Rev.*, 2016, **323**, 60.
13 E. L. Muetterties, J. H. Balthis, Y. T. Chia, W. H. Knoth and H. C. Miller, *Inorg. Chem.*, 1964, **3**, 444.
14 S. Giri, S. Behera and P. Jena, *Angew. Chem., Int. Ed.*, 2014, **53**, 13916.
15 O. Tutusaus, R. Mohtadi, T. S. Arthur, F. Mizuno, E. G. Nelson and Y. V. Sevryugina, *Angew. Chem., Int. Ed.*, 2015, **54**, 7900.
16 T. J. Udovic, M. Matsuo, A. Unemoto, N. Verdal, V. Stavila, A. V. Skripov, J. J. Rush, H. Takamura and S. Orimo, *Chem. Commun.*, 2014, **50**, 3750.
17 T. J. Udovic, M. Matsuo, W. S. Tang, H. Wu, V. Stavila, A. V. Soloninin, R. V. Skoryunov, O. A. Babanova, A. V. Skripov, J. J. Rush, A. Unemoto, H. Takamura and S. Orimo, *Adv. Mater.*, 2014, **26**, 7622.
18 W. S. Tang, A. Unemoto, W. Zhou, V. Stavila, M. Matsuo, H. Wu, S. Orimo and T. J. Udovic, *Energy Environ. Sci.*, 2015, **8**, 3637.
19 W. S. Tang, M. Matsuo, H. Wu, V. Stavila, W. Zhou, A. A. Talin, A. V. Soloninin, R. V. Skoryunov, O. A. Babanova, A. V. Skripov, A. Unemoto, S.-I. Orimo and T. J. Udovic, *Adv. Energy Mater.*, 2016, **6**, 1502237.
20 L. He, H.-W. Li, H. Nakajima, N. Tumanov, Y. Filinchuk, S.-J. Hwang, M. Sharma, H. Hagemann and E. Akiba, *Chem. Mater.*, 2015, **27**, 5483.
21 Y. Sadikin, M. Brighi, P. Schouwink and R. Černý, *Adv. Energy Mater.*, 2015, **5**, 1501016.
22 W. S. Tang, M. Matsuo, H. Wu, V. Stavila, A. Unemoto, S. Orimo and T. J. Udovic, *Energy Storage Mater.*, 2016, **4**, 79.
23 W. S. Tang, K. Yoshida, A. V. Soloninin, R. V. Skoryunov, O. A. Babanova, A. V. Skripov, M. Dimitrievska, V. Stavila, S. Orimo and T. J. Udovic, *ACS Energy Lett.*, 2016, **1**, 659.
24 B. Bonnetot, H. Mongeot, A. Aboukhassib and F. Lefebvre, *Inorg. Chim. Acta*, 1992, **193**, 21.
25 N. Verdal, J.-H. Her, V. Stavila, A. V. Soloninin, O. A. Babanova, A. V. Skripov, T. J. Udovic and J. J. Rush, *J. Solid State Chem.*, 2014, **212**, 81.
26 A. Ponrouch, E. Marchante, M. Courty, J.-M. Tarascon and M. R. Palacín, *Energy Environ. Sci.*, 2012, **5**, 8572.
27 J. B. Varley, K. Kweon, P. Mehta, P. Shea, T. W. Heo, T. J. Udovic, V. Stavila and B. C. Wood, *ACS Energy Lett.*, 2017, **2**, 250.
28 E. L. Muetterties, R. E. Merrifield, H. C. Miller, W. H. Knoth and J. R. Downing, *J. Am. Chem. Soc.*, 1962, **84**, 2506.
29 D. Sethio, L. M. Lawson Daku and H. Hagemann, *Int. J. Hydrogen Energy*, 2016, **41**, 6814.
30 N. Verdal, T. J. Udovic, V. Stavila, W. S. Tang, J. J. Rush and A. V. Skripov, *J. Phys. Chem. C*, 2014, **118**, 17483.
31 A. V. Soloninin, M. Dimitrievska, R. V. Skoryunov, O. A. Babanova, A. V. Skripov, W. S. Tang, V. Stavila, S. Orimo and T. J. Udovic, *J. Phys. Chem. C*, 2017, **121**, 1000.
32 J. H. Morris, H. J. Gysling and D. Reed, *Chem. Rev.*, 1985, **85**, 51.
33 F. Han, Y. Zhu, X. He, Y. Mo and C. Wang, *Adv. Energy Mater.*, 2016, **6**, 1501590.